23rd International Conference on Renewable Energies and Power Quality (ICREPQ'25)
Tenerife (Spain), 25th to 27th June 2025
Renewable Energy and Power Quality Journal (RE&PQJ)
ISSN 2172-038 X, Volume No.23, September 2025

Stability Analysis of Grid-following Converters in Power Systems Depending on Grid Stiffness

S. Delgado-Sánchez[1], J. L. Rodríguez-Amenedo[1] and S. Arnaltes[1]

[1] Universidad Carlos III de Madrid, ROR: https://ror.org/03ths8210
Departamento de Ingeniería Eléctrica, Avenida de la Universidad, 30 – Leganés, 28911 Madrid (Spain)
First author ORCID: https://orcid.org/0009-0005-8237-7614

Abstract. The integration of renewable energy sources in power systems has become a stability challenge. Their connection is made via power electronics, mostly using a grid-following control scheme. However, it has been proven that this type of control raises instability problems when they are connected to weak grids. This paper focuses on analyzing the stability of grid-following converters when connected to grids with different stiffness using frequency analysis. Firstly, an assessment of the converter's passivity indicates the frequency range where the grid stability can be compromised. Then, a time-domain simulation shows how the converter responds to a voltage dip in each case. Finally, the frequency-domain impedance on the small-signal model reconfirms the previously obtained results. The conclusions support the theory explained and point possible future applications.

Key words. Grid-following converter, weak grid, stability, passivity, impedance stability analysis.

1. Introduction

Nowadays, the electrical energy sector is transitioning from carbon-based generation, which accelerates climate change, to clean generation, such as wind, solar and hydroelectric resources, among others. Their integration into power systems is done by means of power electronic converters, referred as Inverter-based Resources (IBRs). These power converters have different properties that divert from those of traditional synchronous generators (SGs). For example, they lack inertia, which stabilizes the frequency in the short term when contingencies take place in SG-dominated systems [1], [2].

Two main control strategies can be implemented in power converters: grid-following (GFL) and grid-forming (GFM) control. The former is commonly used in the connection of renewable energy sources, such as photovoltaic and wind generation, in power systems. It synchronizes with the grid by measuring its voltage angle via a phase-locked loop (PLL), thus behaving as a current source. On the other hand, GFM converters can be represented as voltage sources because they impose the frequency of the grid voltage [1], [3], [4]. They are designed to emulate the operation of SGs, adding the characteristics of a necessary virtual inertia [5]. Moreover, GFM converters have the ability to operate in islanded mode, unlike GFL [6]. Nowadays, there are countless studies that compare both controls, and it has been demonstrated that power systems become dynamically unstable when the amount of SGs substituted by GFL converters increases [7]. Another fundamental aspect of investigation is how both mentioned controls operate in terms of grid strength. It is well-known that the integration of GFL converters in power systems results in dynamic instability when connected to weak grids [8].

The aim of this paper is to demonstrate this last statement by varying the grid inductance of a GFL-grid system using the impedance method. With this goal in mind, a series of experiments are proposed: converter's passivity analysis, a voltage dip test, obtaining the eigenvalues of the whole system and, finally, an impedance stability analysis by the small-signal model.

This document is organized as follows: the first section corresponds to a description of the addressed inverter, the second one defines the methodology followed to analyze the frequency-domain response and, finally, the last section presents the results obtained and its discussion. A conclusion is included at the end of this paper to group together the main concepts and results obtained.

2. Grid-following converters

As explained in the Introduction, GFL converters set the output current by measuring the voltage angle. They synchronize via a PLL, which measures the grid voltage and obtains its angle to place the *d-q* reference axes. Specifically, it sets the *q* component of the voltage to zero via a proportional-integral (PI) regulator [9]. Fig. 1 describes its model by including the PLL synchronization and control loops.

It has been demonstrated that this type of inverter control produces grid instability when connected to weak grids, i.e., large impedance systems [10] or low Short-Circuit Ratio (SCR). Under these circumstances, a perturbation in the grid current significantly impacts its voltage which then affects the PLL [11], giving rise to the well-known stability

problems. For example, in [12] there is an evaluation of the effect of SCR in PLL-based converters. A widely used technique to study the power system stability is the impedance stability analysis, which calculates the grid and the converter impedance viewed from a point of common coupling (PCC). Subsequently, the system is considered stable if they meet Nyquist criterion [13]. However, the authors of [14] consider another approach and they verify what is called the *passivity* of GFL converters.

3. Methodology

This section is divided into two subsections. The first one gives a brief explanation of the impedance stability criterion, and the second one the definition of a passive system.

A. Impedance stability analysis

As previously mentioned, this technique consists in dividing any power system into two subsystems to calculate their impedances in the frequency-domain. Fig. 2 represents both subsystems as the Norton and Thevenin equivalent, respectively [13], where the grid is addressed with the subscript *g* and the converter, with *c*. The output voltage is defined as

$$V(s) = \frac{Z_g(s)I_c(s) + V_g(s)}{1 + \frac{Z_g(s)}{Z_c(s)}} \tag{1}$$

According to equation (1), an electric system is stable if the term $Z_g(s)/Z_c(s)$ satisfies the general Nyquist criterion [15].

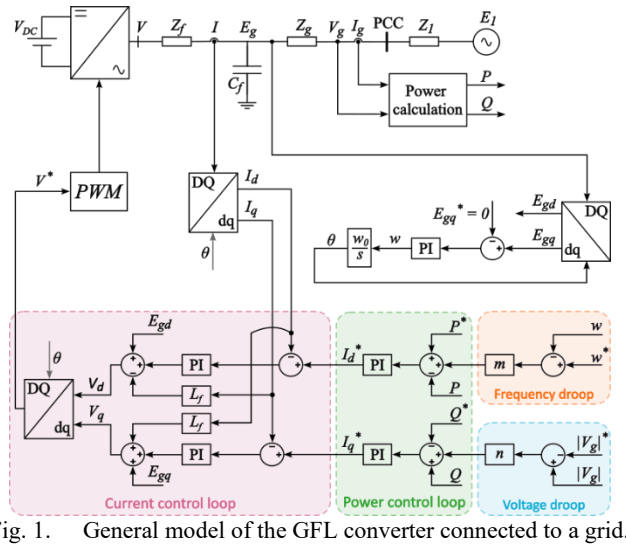

Fig. 1. General model of the GFL converter connected to a grid.

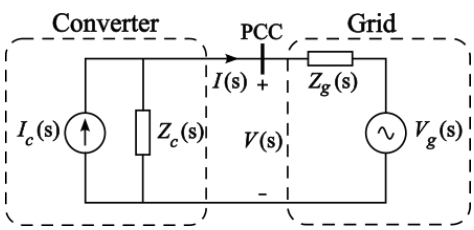

Fig. 2. Small-signal simplification of a grid-connected converter.

A frequency-domain impedance in the *d-q* reference axes is defined as

$$\begin{bmatrix} V_d \\ V_q \end{bmatrix} = \begin{bmatrix} Z_{dd} & Z_{dq} \\ Z_{qd} & Z_{qq} \end{bmatrix} \begin{bmatrix} I_d \\ I_q \end{bmatrix} \tag{2}$$

Where $\boldsymbol{Z_{dq}}$ represents the 2x2 matrix of equation (2), and it can be transformed into the modified sequence domain [15] by

$$\begin{bmatrix} V_p \\ V_n \end{bmatrix} = \begin{bmatrix} Z_{pp} & Z_{pn} \\ Z_{np} & Z_{nn} \end{bmatrix} \begin{bmatrix} I_p \\ I_n \end{bmatrix} \tag{3}$$

Where $\boldsymbol{Z_{pn}}$ represents the 2x2 matrix of equation (3) which is obtained with

$$\boldsymbol{Z_{pn}} = \boldsymbol{A_Z} \cdot \boldsymbol{Z_{dq}} \cdot \boldsymbol{A_Z^{-1}} \tag{4}$$

Where

$$\boldsymbol{A_Z} = \frac{1}{\sqrt{2}} \begin{bmatrix} 1 & j \\ 1 & -j \end{bmatrix} \tag{5}$$

The article [15] defines how to obtain Z_p and Z_n from $\boldsymbol{Z_{pn}}$.

B. Passivity

Another index for evaluating the system stability is through passivity. This is an extensively used guideline for determining how converters perform in the frequency domain [14]. Any converter is non-passive if its conductance is negative at a certain frequency range. In that case, the converter could jeopardize the stability of the system because these frequencies could match a resonance of the grid.

There are two means of analyzing the passivity of converters. The first one is straightforward and consists in checking that the impedance phase lies between ±90°; hence, ensuring its conductance is non-negative. The second approach verifies that the eigenvalues of the sum of the input admittance and its corresponding Hermitian transpose are all positive as the following expression indicates [16].

$$\lambda_{1,2}\left(\boldsymbol{Y_{dq}}(j\omega) + \boldsymbol{Y_{dq}^T}(-j\omega)\right) \geq 0 \qquad \forall\omega \tag{6}$$

Where, $\lambda_{1,2}$ are the eigenvalues, $\boldsymbol{Y_{dq}}(j\omega)$ the admittance and $\boldsymbol{Y_{dq}^T}(-j\omega)$, the Hermitian transpose.

4. Model implementation for simulations

The GFL converter model used throughout the tests is depicted in Fig. 1 together with the configuration of the grid used to evaluate the results: a voltage source behind a complex impedance (defined with the subscript 1). The grid inductance directly determines its stiffness, and thus adjusting the inductance value will achieve the desired SCR.

Both models are implemented into the MATLAB/Simulink with specific scripts to initialize the state-variables for the time-domain simulations. In Simulink, both the converter and grid are modelled in separate masks, as generally depicted in Fig. 3. The GFL mask outputs the capacitor voltage $\vec{E}_g$ by using the PCC voltage $\vec{V}_g$ and the reference variables as inputs (complex power, frequency and voltage module in Fig. 1). Then, the grid mask takes the converter output as an input and returns the PCC voltage, generating a loop. Time-domain simulations achieve flat start-initialization due to the use of the above-mentioned specific scripts.

On the other hand, nonlinear dynamic equations of the GFL converter require the implementation of the small-signal model to perform the frequency-domain simulations.

5. Results and discussion

Both components, GFL converter and grid, are RMS models whose parameters are organized in Table 1. The grid impedance is defined with an added superscript to denote the grid weakness of each test.

It is important to note that the power base (S_b) is equal for both the converter and the grid. However, if it was not the case, the tool is programmed to differentiate both power bases and display correct results. These results are categorized as follows: Section A presents the GFL eigenvalues to check the passivity of the chosen GFL converter model. Section B tests the time-domain response of the converter when a voltage dip is applied. Finally, Section C compares the system stability in the different GFL-grid scenarios by the frequency-domain impedance.

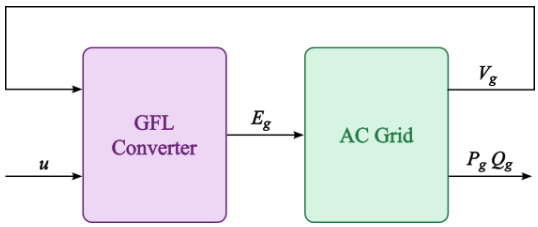

Fig. 3. Connection of the GFL converter and grid models for the time-domain simulation

Table 1. Simulation parameters

Global parameters			
ω_0 (Hz)	50	S_b (MVA)	5
$\vec{V}_g$ (p.u)	1+0j	$\vec{S}_g$ (p.u)	1+0.3j
GFL converter		**Grid**	
$\vec{Z}_g$ (p.u)	0.0027+j0.08	$\vec{Z}_1^1$ (p.u)	0.0002+j0.05
$\vec{Z}_f$ (p.u)	0.0030+j0.15	$\vec{Z}_1^2$ (p.u)	0.0002+j0.13
C_f (p.u)	0.266	$\vec{Z}_1^3$ (p.u)	0.0002+j0.20
Control parameters			
PI controller of the PLL		k_{ps} (p.u)	0.0127
		k_{is} (p.u/s)	0.25
Gain of the frequency and voltage droops		m	10
		n	5
PI controller of the power control loop		k_{pv} (p.u)	0.05
		k_{iv} (p.u/s)	2.5
PI controller of the current control loop		k_{pc} (p.u)	0.01
		k_{ic} (p.u/s)	0.0628

A. *Passivity of the GFL converter model*

This first test evaluates the passivity of the GFL converter. Fig. 4 presents eigenvalues $\lambda_{1,2}$ calculated with expression (6).

λ_{1c} exhibits peak negative values around the fundamental frequency and low negative values in the subsynchronous plane. The higher the negative value of the former, the greater the stability concern, because if these frequencies match a resonance of the grid, the system will be unstable.

B. *Voltage dip*

This time-domain test consists in applying a voltage dip on the grid ($\vec{E}_1$) to analyze the converter response. During the voltage dip, the magnitude lows in 0.8 p.u from t = 1s to t = 1.5s and after, the voltage recovers its initial value. The goal of evaluating the operation of the converter by varying the grid stiffness implies that the test is conducted three times, with the grid impedances defined in Table 1.

Fig. 5 shows that an increase in the grid inductance results in a less damped power and voltage response. It also displays the loss of synchronism after the voltage dip recovery in the weakest grid (L_1 = 0.20 p.u, which becomes SCR = 5), confirming the statement previously introduced and widely studied among investigators.

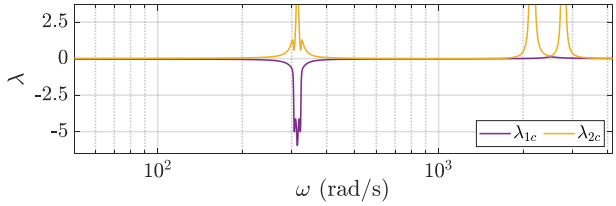

Fig. 4. Eigenvalues obtained to check the passivity of the GFL converter.

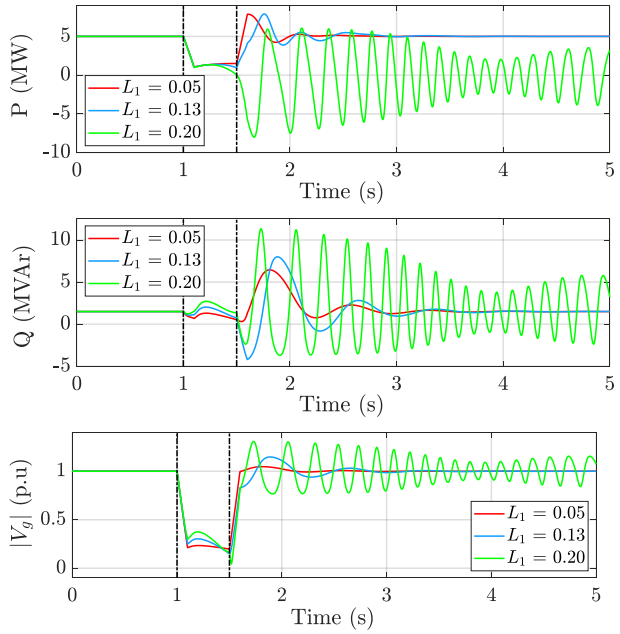

Fig. 5. Active power (up) and reactive power (middle) injected into the grid, and PCC voltage magnitude (down) during the voltage dip simulation.

While the time-domain simulation presents a connection between system stability and grid weakness in GFL converters, more evidence is needed to draw conclusions. For example, the eigenvalues of both systems (converter and grid) will give the oscillatory and damping characteristics of the system and are plotted in Fig. 6.

All the eigenvalues of the system are placed in the negative-real half plane. However, as the grid inductance increases (lower SCR), the real part of its eigenvalues approaches the imaginary axis, becoming less negative and hence, less damped and more oscillatory.

C. Grid and converter frequency-domain impedance

The frequency-domain analysis on small-signal models is the last method of stability validation. As defined in (1), the expression $Z_g(s)/Z_c(s)$ has to meet the Nyquist criterion. However, the frequency-domain impedance is depicted in a Bode plot, and thus the key elements of stability evaluation are the intersection points between both impedance curves.

Fig. 7 presents four positive-impedance Bode plots, corresponding to the three GFL-grid cases examined until now, plus a new example with a grid impedance of $Z_1^4 = 0.0002 + j0.50$ p.u. (SCR = 2). The magnitude subplots show that the weaker the grid becomes, the greater number of intersections between both graphs. Notably, the stiffest grid and the GFL positive impedances do not meet but, from that case forward, synchronous resonances appear, endangering the system stability. Furthermore, the newly introduced case (which corresponds to the weakest grid) presents 4 additional cross points in the supersynchronous range. Ultimately, a close examination of each intersection's phase margin will precisely determine which frequencies lead to instability.

6. Conclusion

The continuous connection of green energy sources via GFL control exposes instability problems in weak grids, as SGs are being replaced by IBRs. For this reason, this paper analyzes the impact of a decreasing SCR in a grid with increasing number of IBRs with GFL control. The system stability successfully verified the last statement not only by performing time-domain simulations, but also by applying the latest stability methods proposed in the scientific community. First, the converter's passivity details the potentially unstable frequency range prior to any other simulation. The frequency-domain impedance analysis delivers a clear pattern of the system stability as the inductance of the grid increases.

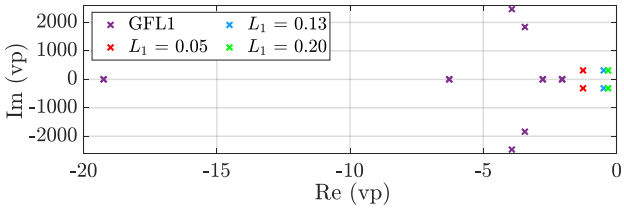

Fig. 6. Eigenvalues of the system.

The simulations studied validate the stability behavior by modelling the simplest grid: a voltage source behind an impedance. For future applications, more complex grids with multiple GFL converters will reveal interaction between controls and bring a more realistic dynamic response. Furthermore, the exponential interest in integrating GFM into power systems raises the need to evaluate its performance with varying grid conditions.

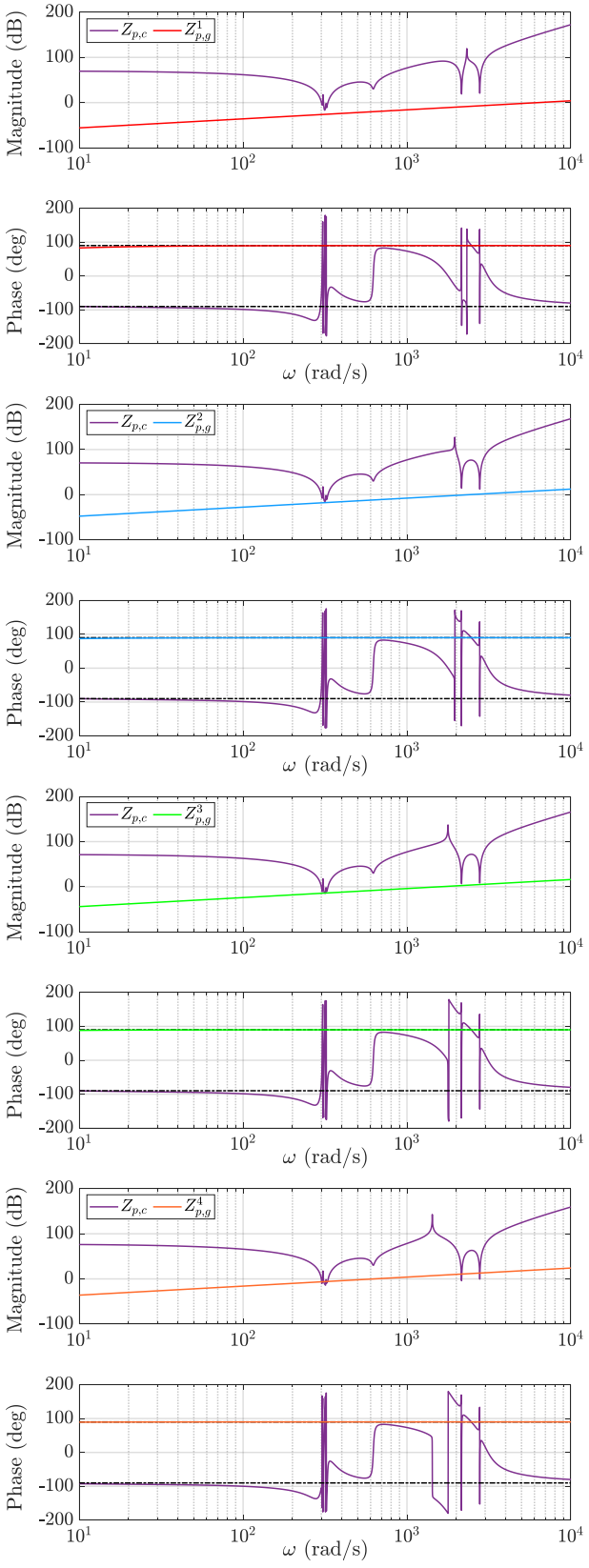

Fig. 7. Positive-sequence impedances of the GFL-grid systems.

Acknowledgement

This work was supported by the Spanish Research Agency under Grant TED2021-130468B-I00 MCIN/AEI/MCIN/AEI/10.13039/ 501100011033. NextGenerationEU/PRTR: CONTRIBUTION OF GRID FORMING CONVERTERS TO POWER SYSTEMS STABILITY AND OPERABILITY WITH HIGH PENETRATION OF RENEWABLE ENERGY SOURCES (GFM-RES).,

Grant PDC2022-133349-I00 funded by MCIN/AEI/10.13039/501100011033 and by the European Union "NextGenerationEU/PRTR". PRUEBA DE CONCEPTO DE CONVERTIDORES FORMADORES DE RED PARA CONTRIBUIR AL SERVICIO DE REPOSICION DEL SISTEMA ELECTRICO

Grant: Acción financiada por la Comunidad de Madrid en el marco del convenio plurianual con la Universidad Carlos III Madrid en su línea de actuación "Excelencia para el Profesorado Universitario". V Plan Regional de Investigación Científica e Innovación Tecnológica 2016-2020

References

[1] B. Kroposki *et al.*, "Achieving a 100% Renewable Grid: Operating Electric Power Systems with Extremely High Levels of Variable Renewable Energy," *IEEE Power and Energy Magazine*, vol. 15, no. 2, pp. 61–73, Mar. 2017, doi: 10.1109/MPE.2016.2637122.

[2] F. Milano, F. Dorfler, G. Hug, D. J. Hill, and G. Verbic, "Foundations and Challenges of Low-Inertia Systems (Invited Paper)," in *2018 Power Systems Computation Conference (PSCC)*, IEEE, Jun. 2018, pp. 1–25. doi: 10.23919/PSCC.2018.8450880.

[3] T. Ackermann, T. Prevost, V. Vittal, A. J. Roscoe, J. Matevosyan, and N. Miller, "Paving the Way: A Future Without Inertia Is Closer Than You Think," *IEEE Power and Energy Magazine*, vol. 15, no. 6, pp. 61–69, Nov. 2017, doi: 10.1109/MPE.2017.2729138.

[4] W. Du *et al.*, "Modeling of Grid-Forming and Grid-Following Inverters for Dynamic Simulation of Large-Scale Distribution Systems," *IEEE Transactions on Power Delivery*, vol. 36, no. 4, pp. 2035–2045, Aug. 2021, doi: 10.1109/TPWRD.2020.3018647.

[5] D. B. Rathnayake *et al.*, "Grid Forming Inverter Modeling, Control, and Applications," *IEEE Access*, vol. 9, pp. 114781–114807, 2021, doi: 10.1109/ACCESS.2021.3104617.

[6] J. Rocabert, A. Luna, F. Blaabjerg, and P. Rodríguez, "Control of Power Converters in AC Microgrids," *IEEE Trans Power Electron*, vol. 27, no. 11, pp. 4734–4749, Nov. 2012, doi: 10.1109/TPEL.2012.2199334.

[7] D. Pattabiraman, R. H. Lasseter, and T. M. Jahns, "Comparison of Grid Following and Grid Forming Control for a High Inverter Penetration Power System," in *2018 IEEE Power & Energy Society General Meeting (PESGM)*, IEEE, Aug. 2018, pp. 1–5. doi: 10.1109/PESGM.2018.8586162.

[8] M. Davari and Y. A.-R. I. Mohamed, "Robust Vector Control of a Very Weak-Grid-Connected Voltage-Source Converter Considering the Phase-Locked Loop Dynamics," *IEEE Trans Power Electron*, vol. 32, no. 2, pp. 977–994, Feb. 2017, doi: 10.1109/TPEL.2016.2546341.

[9] Y. Li, Y. Gu, and T. C. Green, "Revisiting Grid-Forming and Grid-Following Inverters: A Duality Theory," *IEEE Transactions on Power Systems*, vol. 37, no. 6, pp. 4541–4554, Nov. 2022, doi: 10.1109/TPWRS.2022.3151851.

[10] D. Dong, B. Wen, D. Boroyevich, P. Mattavelli, and Y. Xue, "Analysis of Phase-Locked Loop Low-Frequency Stability in Three-Phase Grid-Connected Power Converters Considering Impedance Interactions," *IEEE Transactions on Industrial Electronics*, vol. 62, no. 1, pp. 310–321, Jan. 2015, doi: 10.1109/TIE.2014.2334665.

[11] X. Wang, M. G. Taul, H. Wu, Y. Liao, F. Blaabjerg, and L. Harnefors, "Grid-Synchronization Stability of Converter-Based Resources—An Overview," *IEEE Open Journal of Industry Applications*, vol. 1, pp. 115–134, 2020, doi: 10.1109/OJIA.2020.3020392.

[12] J. Z. Zhou, H. Ding, S. Fan, Y. Zhang, and A. M. Gole, "Impact of Short-Circuit Ratio and Phase-Locked-Loop Parameters on the Small-Signal Behavior of a VSC-HVDC Converter," *IEEE Transactions on Power Delivery*, vol. 29, no. 5, pp. 2287–2296, Oct. 2014, doi: 10.1109/TPWRD.2014.2330518.

[13] J. Sun, "Impedance-Based Stability Criterion for Grid-Connected Inverters," *IEEE Trans Power Electron*, vol. 26, no. 11, pp. 3075–3078, Nov. 2011, doi: 10.1109/TPEL.2011.2136439.

[14] L. Harnefors, X. Wang, A. G. Yepes, and F. Blaabjerg, "Passivity-Based Stability Assessment of Grid-Connected VSCs—An Overview," *IEEE J Emerg Sel Top Power Electron*, vol. 4, no. 1, pp. 116–125, Mar. 2016, doi: 10.1109/JESTPE.2015.2490549.

[15] A. Rygg, M. Molinas, C. Zhang, and X. Cai, "A Modified Sequence-Domain Impedance Definition and Its Equivalence to the dq-Domain Impedance Definition for the Stability Analysis of AC Power Electronic Systems," *IEEE J Emerg Sel Top Power Electron*, vol. 4, no. 4, pp. 1383–1396, Dec. 2016, doi: 10.1109/JESTPE.2016.2588733.

[16] A. Rygg and M. Molinas, "Apparent Impedance Analysis: A Small-Signal Method for Stability Analysis of Power Electronic-Based Systems," *IEEE J Emerg Sel Top Power Electron*, vol. 5, no. 4, pp. 1474–1486, Dec. 2017, doi: 10.1109/JESTPE.2017.2729596.